A model for the dynamics of sandpile surfaces

J.-P. Bouchaud, M. Cates, J. Ravi Prakash, S. Edwards

Classification
Physics Abstracts
46.10 — 05.40

A model for the dynamics of sandpile surfaces

J.-P. Bouchaud (*), M. E. Cates, J. Ravi Prakash (**) and S. F. Edwards

Cavendish Laboratory, Madingley Road, Cambridge CB3 0HE, U.K.

(Received 31 March 1994, accepted in final form 30 June 1994)

Abstract . — We propose a new continuum description of the dynamics of sandpile surfaces, which recognizes the existence of two populations of grains: immobile and rolling. The rolling grains are carried down the slope with a constant drift velocity and have a certain dispersion constant. We introduce a simple bilinear approximation for the interconversion process, which represents both the random sticking of rolling grains (below the angle of repose), and the dislodgement of immobile grains by rolling ones (for greater slopes). We predict that the mean downhill motion of rolling grains causes surface features to move *uphill*; shocks can arise at large amplitudes. Our equations exhibit a second critical angle, larger than the angle of repose, at which the surface of a tilted immobile sandpile first becomes unstable to an infinitesimal perturbation. Our model is used to interpret the results of rotating-drum experiments. We study the long time behaviour of our equations in the presence of noise. For an initially rough surface at the repose angle, with no incident flux and an initially constant rolling grain density, the roughness decays to zero in time with an exponent found from a linearized version of the model. In the presence of spatiotemporal noise, we find that the interconversion nonlinearity is irrelevant, although roughness now becomes large at long times. However, the Kardar-Parisi-Zhang nonlinearity remains relevant. The behaviour of a sandpile with a steady or noisy input of grains at its apex is also briefly considered. Finally, we show how our phenomenological description can be derived from a discretized model involving the stochastic motion of individual grains.

1. Introduction and model.

The physics of granular media (powders) is interesting from many standpoints, not least because of its obvious practical and engineering importance [1, 2]. In this paper we study theoretically the surface evolution of a sandpile, whose mean slope is close to the angle of repose. This problem has recently gained the status of a paradigm in the physics literature: sandpiles were proposed as a prototype of 'open dissipative systems' and predicted to exhibit 'self-organized

(*) *Present address:* Service de Physique de l'Etat Condensé, CEA, Orme des Merisiers, 91191 Gif sur Yvette Cedex, France.
(**) *Present address:* Institut für Polymere, ETH-Zentrum, CH-8092, Zurich, Switzerland.

criticality', that is, scale- and time-invariant dynamics [3]. Thus, for example, if grains are dropped onto the centre of a sandpile supported by a plate (Fig. 1), the slope fluctuates in time, as does the flux of grains leaving at the lower edge; theories of self-organized criticality predict power-law spectra for (say) the distribution of avalanche sizes. This proposal has lead to a series of original and interesting experiments [4-7], as well as a great number of theoretical and numerical works [8-10]. However, there is evidence that sandpiles do not usually show self-organized criticality [11]. Often the behaviour is more reminiscent of properties of an equilibrium system close to a first order phase transition (displaying hysteresis [12]) rather than a second order transition (displaying power-law behaviour) as suggested by theory.

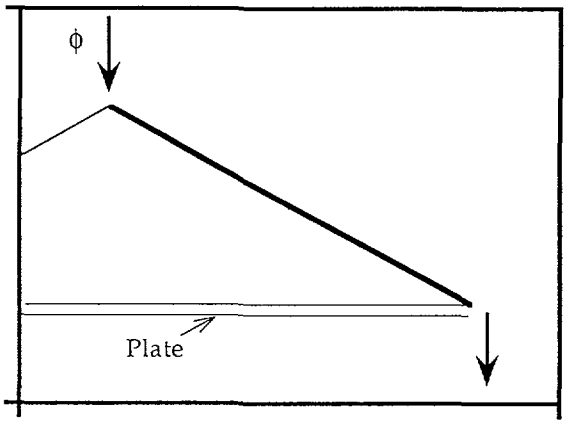

Fig. 1. — Typical situation considered in this paper: a sandpile on a plate, fed or disturbed from the top or from the bottom; the grains are supposed to be extracted from the pile when they reach the edge of the plate.

In the remainder of section 1, we discuss previous approaches to the problem and motivate a new phenomenologial treatment involving two coupled hydrodynamic variables. We discuss with some care the simplifying assumptions we have made, and identify scope for variation in these assumptions. In section 2 we use our model to consider simple (noise-free) problems in sandpile dynamics, and in section 3 turn to problems involving noise. Finally in section 4 we show how our continuum equations for sandpile motion emerge naturally from a microscopic description involving the stochastic motion of individual grains. Our conclusions are summarized briefly in section 5.

1.1 PREVIOUS APPROACHES. — Various models have been proposed to describe the time evolution of the height of a sandpile: for example one can set up a discrete cellular automaton in which a local threshold slope is introduced, above which 'avalanches' are initiated [3, 13]. Soon after these cellular automaton models were investigated, Hwa and Kardar [14] proposed a continuum description of the same problem. Their philosophy was to write down the most general nonlinear local dynamical equation compatible with the symmetries of the system, selecting nonlinear terms on the basis of "relevance" criteria determined (essentially) by dimensional analysis. On these grounds, Hwa and Kardar proposed that 'sandpiles' [14] should

be governed an anisotropic 'Driven Diffusion Equation':

$$\frac{\partial h(\mathbf{r},t)}{\partial t} = \nu\partial_x^2 h(\mathbf{r},t) + \nu_\perp \partial_\perp^2 h(\mathbf{r},t) - \mu\partial_x(h(\mathbf{r},t)^2) + \eta(\mathbf{r},t) \tag{1}$$

where $h(\mathbf{r},t)$ is the height above a point $\mathbf{r}$ in the plane; a background slope, presumed equal to the angle of repose, has been subtracted. The spatial variable x is the component of $\mathbf{r}$ along the downward axis of the sandpile; ν and $\nu_\perp$ are effective surface tensions; and μ controls the strength of the non-linear term, which was argued to capture the important aspects of any threshold effects. Finally, $\eta(\mathbf{r},t)$ is a noise term describing the random addition of grains.

The strength of this phenomenological approach lies partly in its avoidance of the complexity of the full problem, which might in principle require a description of the bulk of the sandpile. Alternative phenomenological descriptions have also been proposed for this and other, closely related, problems such as the surface of a sandpile vibrated from below [15, 16]. Often one is interested in the scaling behaviour which controls the properties of the system at long times; in the presence of noise, the initial condition is then unimportant. The long time properties of equation (1) can be studied using theoretical or numerical approaches [17, 14, 18, 19], to obtain information on the response and correlation functions. One finds, for both two dimensional and three dimensional sandpiles, 'superdiffusive dynamics' (the correlation length increasing faster than $t^{1/2}$) and a stationary profile that is asymptotically flat (i.e., height fluctuations that saturate at large separations).

Noisy non-linear equations, such as the Hwa-Kardar equation, are certainly of great interest from a physics perspective (see e.g. Refs. [20, 18, 14, 21]), especially when they lead to criticality and scaling laws in the long time limit. Nonetheless, from the point of view of understanding sandpiles, it seems desirable that a phenomenological model should also describe simpler situations, which include the deterministic evolution of a sandpile in the absence of noise. This would enable the basic model to be validated before the added complexity of noise terms is introduced. In any case, several aspects of the Hwa-Kardar treatment can be criticized, as follows.

(i) Although the whole argument is based on symmetry considerations, equation (1) violates the most natural one, which is translational invariance in h: translating the sandpile upwards should not change its dynamical equation. Hwa and Kardar suggest that this symmetry could be spontaneously broken, although the mechanism remains to us rather obscure.

(ii) Secondly, equation (1) predicts a slow decay (as t^{-1}) of the sandpile surface to zero slope (after subtraction of the repose angle) if the noise is suddenly switched off. We would argue that, in a realistic model, the surface should typically come to rest in a metastable state intermediate between the initial one, and that of zero slope.

(iii) Our third point is of more general scope: symmetry arguments alone are sufficient to construct phenomenological equations *only if one takes into account all the slow variables in the problem.* The presence of a hidden slow (hydrodynamical) variable induces in general long range effects and forbids a naive local gradient expansion in the height variable.

1.2 A MODEL WITH TWO DEGREES OF FREEDOM. — In the case of sandpiles, we believe that the local height $h(\mathbf{r},t)$ is not the only hydrodynamical variable. Instead, the grains can be in two different states: either immobile or rolling downwards. We thus suggest that a suitable hydrodynamical description should include, along with h (which is the height of a stack of immobile grains), the local density of rolling grains $\mathcal{R}$. These must be coupled dynamically by an interaction term, allowing for the conversion of rolling grains to sticking grains and *vice versa*. In this section we derive appropriate coupled equations for these quantities on a purely

phenomenological basis. (Their relation to a more fundamental microscopic formulation is explored in Sect. 4). Since it deals only with surface variables, our description does not, of course, take into account any long-range effects mediated by the stress field in the bulk of the medium, which might be significant in some situations.

The insight that two order parameters, rather than one, would better describe the evolution of sandpiles is that of Mehta [16], who introduced a model with two coupled variables in the context of modelling vibrated sandpiles. Mehta's two variables were not h and $\mathcal{R}$, however; they described two different aspects of surface roughness, coupled to the dynamics of collective and single-particle rearrangements [16]. We believe our own choice is more directly related to the physics of the underlying problem.

From now on, we shall for simplicity work in one projected dimension (i.e. we consider two-dimensional sandpiles whose height $h(x,t)$ depends on one spatial variable). The generalisation of the following equations to higher dimensions is immediate (though their solution is often not). We first propose that the rolling grains are governed by a convective diffusion equation of the following form:

$$\dot{\mathcal{R}}(x,t) = -\partial_x(v\mathcal{R}(x,t)) + \partial_x(\mathcal{D}\partial_x\mathcal{R}(x,t)) + \Gamma(\mathcal{R}(x,t), h(x,t)) \tag{2}$$

where $\mathcal{R}\mathrm{d}x$ is the number of rolling grains between x and $x + \mathrm{d}x$, v is the drift velocity of the rolling grains downwards along x; $\mathcal{D}$ is a diffusion (or dispersion) constant. For simplicity, we treat both v and $\mathcal{D}$ as constants in time and space. As discussed in section 2 below, one can gain indirect information on these quantities from 'rotating drum' experiments.

The term Γ accounts for the conversion of immobile grains into rolling grains, and *vice versa*. We shall construct Γ with the help of the following physical considerations:

(a) We assume that an immobile grain cannot spontaneously start rolling unless it is dislodged by an already rolling grain. This seems reasonable close to the angle of repose, although in principle at some larger angle a static grain could cease to be supported by those below it, and start rolling. However, to create this condition in the absence of rolling grains clearly requires an external perturbation, such as an imposed tilt of the entire sandpile. (We return to this issue in our discussion of the Bagnold angle in Sect. 2.2).

(b) The local slope $-\partial_x h$ of the sandpile must exceed a critical value S_c (which we associate with the angle of repose) for the dislodging process to be effective. For convenience we can subtract off a background slope, so that S_c is zero, unless otherwise stated. With this choice, the gradient of h is everywhere small and we need not distinguish between gradients and angles. By convention we consider piles that are decreasing in height with increasing x (sloping down to the right); thus $\partial_x h > 0$ corresponds to a surface less steep than the angle of repose.

(c) If the local slope is less than the critical slope S_c (i.e., $\partial_x h > 0$) then rolling grains will tend to stick to the surface, thus being converted into immobile grains. This occurs independently for each rolling grain, and hence at a rate proportional to $\mathcal{R}(x,t)$ itself.

(d) If $\partial_x h = S_c$, but $\partial_x^2 h \neq 0$, then conversion acts to reduce the local curvature of the surface (filling in hollows and eroding bumps) again at a rate proportional to $\mathcal{R}$.

The simplest form of Γ exhibiting the above four properties is the following:

$$\Gamma(h,\mathcal{R}) = -\mathcal{R}[\gamma\partial_x h + \kappa\partial_x^2 h] \tag{3}$$

with $\gamma > 0$ and $\kappa > 0$. This expression, though nonlinear, depends linearly on each of $\mathcal{R}$ and h, a choice which offers great advantages in analytical work. This major simplification corresponds to assuming that, for a given rolling grain density, the rate of deposition or dislodgement of static grains varies smoothly from positive to negative as the slope passes through S_c. In

principle this should not be true (except if there is a 'particle-hole' symmetry of the kind discussed in Ref. [14]): instead, one should introduce two coefficients γ^+ and γ^- for slopes above and below the critical value (likewise also for κ). However, this simplifying assumption seems to us reasonable (but see below Sect. 1.3, viii); when it holds, our choice of Γ becomes simply the first term of a Taylor expansion (for $\mathcal{R}$ and h small).

Having chosen Γ, we can at once write down an equation for the height $\dot{h}(x,t)$ of the sandpile (in suitable units), which we define to include only immobile grains, as follows:

$$\dot{h} = -\Gamma = \mathcal{R}(x,t)[\gamma \partial_x h + \kappa \partial_x^2 h] \tag{4}$$

so that the total number of grains $(h+\mathcal{R})$ is conserved locally. Since Γ is linear in $\mathcal{R}$, it follows from equation (4) that in the absence of rolling grains, the surface is 'frozen' in a metastable state, and is incapable of spontaneous rearrangement. A static system which is perturbed (so that some rolling grains are generated) will typically evolve for a short time but then immobilize in a new state as the rolling grains come to rest. This metastability is a characteristic feature of powders, and we believe that it is important to incorporate it, at least qualitatively. (As noted previously, this feature is not easily captured in the Hwa-Kardar approach.) We shall see later that it can lead to hysteresis and other interesting effects.

Equations (2-4) comprise the basic phenomenological theory with which we aim to describe the surface evolution of sandpiles. Before applying the model to some interesting situations, we make some further comments about the structure of the model, and possible variations of it (either in the equations themselves, or in their interpretation).

1.3 VARIOUS REMARKS. — (i) Equations (2, 4) are invariant when $h \to h + \text{const.}$, as they should be. The total number of grains is conserved since $\partial(h+\mathcal{R})/\partial t$ can be written as the divergence of a current. Note, however, that the conservation of grain number only implies volume conservation if the underlying powder has a fixed density.

(ii) The actual height of the sandpile may of course be defined to include the rolling grains. Since in the moving phase powders expand, the true height of the sandpile reads $\mathcal{H} = h + \alpha\mathcal{R}$ with $\alpha > 1$ an unknown parameter of the theory. For simplicity, we consider only the underlying height h in what follows.

(iii) The term in κ in equation (4) is physically crucial. This term alone allows surface features to be smoothed, rather than simply convected from one place to another (see Sect. 2 below) under the action of rolling grains. For example, one can prove that for $\kappa = 0$ the probability distribution of the heights of local maxima in h is conserved in time.

(iv) In contrast, the model obtained by setting $\mathcal{D} = 0$ in equation (2) remains sensible, and shares several major properties with the full equations. However, this diffusive term represents the only means by which rolling grains can propagate backward up the slope of a sandpile. This propagation turns out to be essential to the description of hysteresis phenomena (see Sect. 2), and so we retain $\mathcal{D} > 0$ in what follows. More realistically, this dispersive term could arise, not by any individual grains actually moving uphill, but rather from the fact that a rolling grain can dislodge grains a little above it (or below it) on the slope. A more detailed model of that process would require $\mathcal{D}$ to depend on $\partial_x h$. (The resulting terms, such as $\partial_x^2 \mathcal{R} \partial_x h$, could be viewed as contributions to Γ.) For simplicity we study only the simplest version (constant $\mathcal{D}$) in this paper.

(v) Several other physical effects could complicate these equations by adding new nonlinear terms. For example, the velocity of rolling grains (as well as the diffusion constant, see (iv) above) might depend on the local slope and also on the local density of moving grains,

giving extra terms in equation (2). However, we believe that equations (2-4) already capture the essential physics of the problem (which might be obscured by introducing too many phenomenological parameters).

(vi) In the presence of a incident flux of grains (deterministic or random), an input term $\eta(x,t)$ should of course be added. It is not totally obvious, however, whether $\eta(x,t)$ should be added to equation (2), or to equation (4), or to both. Arguably this depends on the properties of the grains themselves. In the case of "soft grains" $\eta(x,t)$ should presumably be added to the $\dot{h}(x,t)$ equation, since these grain will generally stick upon landing. In the case of hard elastic grains, the added grains will primarily contribute in the rolling grain density, and hence $\eta(x,t)$ should be added to the $\dot{\mathcal{R}}$ equation.

(vii) If the average incident flux of grains $\langle\eta\rangle$ is non-zero (as expected physically) one should follow Kardar, Parisi and Zhang (KPZ) [20] and add a term proportional to $\langle\eta\rangle(\partial_x h)^2$, which takes into account the dependence of the flux of particles on the local orientation of the surface [20, 18, 21]. Such a term is clearly appropriate for soft particles (added directly to h); its inclusion is not so transparent for hard grains (when the incident flux is added to $\mathcal{R}$).

(viii) A similar term may also arise from the asymmetry between dislodgement and sticking processes. The constant coefficient γ in equation (3) could be replaced by $\gamma_0+\gamma_1\partial_x h$ to account for this asymmetry, either as the next term in a series expansion, or to mimic the discontinuous case when $\gamma^+ \neq \gamma^-$. This contributes to Γ a term in $\mathcal{R}(\partial_x h)^2$, which reduces to a KPZ term in equation (4) if $\mathcal{R}$ is weakly fluctuating.

(ix) Finally, we note that although our arguments are couched in terms of "rolling" grains, very similar considerations can be used to construct a model in which dislodged grains do not roll, but bounce loosely along the sand-pile surface. This may require a distributed energy source such as external vibration of the pile, though for large elastic grains (such as boulders in a rockfall), that does not seem to be necessary. Similar behaviour occurs when an external convection (such as wind) is applied to a roughly horizontal surface. In this situation there will be large changes in the interconversion constants γ and κ. Otherwise, it is arguable that the basic structure of the equations is the same; if so, many or our results can be carried over to these problems.

2. Deterministic examples.

We shall now analyse our phenomenological equations in some physically motivated situations. In this section, simple deterministic evolutions (such as an isolated bump, Sect. 2.1) are considered; noisy situations are deferred to section 3. This section of the paper is mostly qualitative, but our arguments are illustrated and supported by some numerical solutions of the governing equations. One interesting outcome of our analysis (Sect. 2.2) is that an immobile sandpile remains stable to small perturbation until a 'spinodal' critical slope S_d, strictly larger than S_c (the repose angle) is reached. We shall also discuss in section 2.3 and 2.4 the characteristic relaxation time scales pertaining to 'rotating drum' experiments [4, 7], and show how to estimate on this basis the model parameters v and $\gamma\mathcal{D}$. Section 2.5 concerns a sandpile with a point source of incident flux.

2.1 EVOLUTION OF A BUMP AND OF A SINUSOID. — Let us first look qualitatively at the case where a single small bump sits in the middle of an otherwise flat surface (at angle S_c), with a constant rolling grain density $\mathcal{R}_0$. Equation (4) then reveals that the bump propagates *uphill* with velocity $v_h = \gamma\mathcal{R}_0$. (It also undergoes spreading due to the dispersion term.) For a sandpile, this interesting behaviour reflects the fact that rolling grains deposit on the flatter

(uphill) part of the bump, and erode the steeper (downhill) part, resulting in a net uphill translation. Hence the surface structure is convected upwards by the action of rolling grains; this is a generic feature of the model. The effect is similar to the well known fact that traffic jams propagate in the opposite direction to the flow of cars [22]. In contrast, a curious feature of the Hwa-Kardar formulation, equation (1), is that bumps might travel either upwards or downwards depending on their absolute height.

Measurements of the uphill convection speed could in principle be used to extract the value of γ from an experiment where $\mathcal{R}_0$ as well as the upwards velocity are measured. Experimentally, uphill-travelling "surface waves" have recently been observed in sandpiles vibrated from below, although the physics here may be more complicated, since bulk convective motions of the pile were apparently involved [23].

Suppose now that one now starts with a sinusoidal profile, $\dot{h}(x,t) = h_0 \sin(2\pi x/\lambda)$, with an initially constant rolling grain density $\mathcal{R}_0$. If h_0 is small enough, the variations of $\mathcal{R}(x,t)$ due to the evolution of $\dot{h}(x,t)$ will be negligible; the oscillatory profile will be convected uphill and decay exponentially in time (due to the diffusion term in Eq. (4)), with a relaxation time $\tau_\lambda = \lambda^2/\mathcal{R}_0\kappa$. The uphill motion can only be observed if $v_h\tau_\lambda > \lambda$, i.e. when $\lambda\gamma/\kappa > 1$. If on the other hand h_0 is not small, shocks can appear. This has been confirmed numerically (see Fig. 2); the numerical scheme used is described in the Appendix. These shocks arise because regions where $|\partial_x h|$ is initially larger will generate more rolling grains, thereby enhancing their effective upwards velocity. Once a shock has appeared, it becomes the dominant cause of the relaxation of the profile. The gradient in the shock is of order h/a, with a is the shock-width (of order the grain size) and the relaxation rate in the presence of shocks is then found to be $\simeq a^2/\mathcal{R}_0\kappa$.

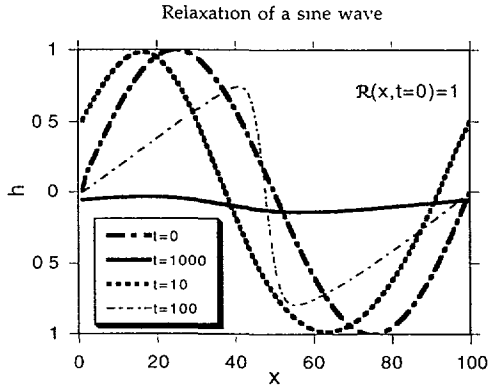

Fig. 2. — Numerical results for an initial sinusoidal height profile with a constant rolling grain density $\mathcal{R}_0$, at various times. In this case, the initial amplitude was high enough to produce shocks at intermediate times.

2.2 HYSTERESIS; MAXIMUM ANGLE OF STABILITY. — Next we consider the situation of figure 3, where a sandpile is prepared in a metastable state, with $\partial_x h(x,0) = -S_0 < 0$ [24], but with no rolling grains. (This can be done by simply tilting the base of a sandpile which was at its angle of repose.) As we have already emphasized, since no rolling grains are present, this situation does not evolve with time. However, imagine now that one slightly perturbs this initial state by creating a small number of rolling grains at the *lower* edge of the pile. (This

could be done by dislodging a few grains so as to spill over the lip of the supporting plate, or by briefly opening a small hole there.) Interestingly, the subsequent evolution will depend critically on the initial slope perturbation S_0, as shown by the following argument.

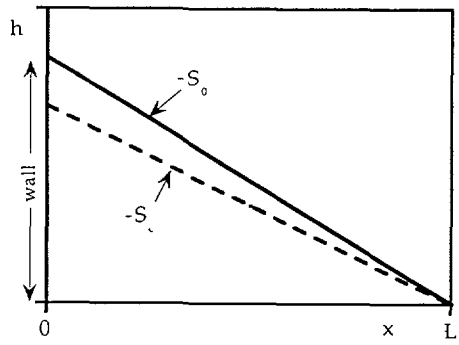

Fig. 3. — Initial metastable configuration of a sandpile, with slope S_0 larger than the nominal stable slope S_c. This configuration is then perturbed by a small amount of rolling grains, introduced either at the bottom or at the top of the pile.

If, at time zero, a small pulse of rolling grains $\mathcal{R}(x',0) = \Delta\mathcal{R}_0\,\delta(x'-x)$ is created at site x, then two opposite effects will come into play:

(i) Firstly, the rolling grains are convected away downhill, tending to restabilize the profile near x in a new frozen state. The effect of this can be isolated in equation (2) by excluding the interconversion term Γ; we find that the density of rolling grains at x after time t evolves as

$$\mathcal{R}(x,t) = \frac{\Delta\mathcal{R}_0}{\sqrt{4\pi\mathcal{D}t}}\exp[-v^2t/4\mathcal{D}] \tag{5}$$

Note that the dispersion process, governed by $\mathcal{D}$, is the only factor limiting the effectiveness of convection at carrying away the perturbation: if $\mathcal{D} \to 0$, the rolling grain density at x falls to zero instantaneously.

(ii) Secondly, the rolling grains cause dislodgement which acts as a source of new rolling grains. From equation (2), one finds that in the absence of convection or diffusion ($v = \mathcal{D} = 0$), $\mathcal{R}(x,t)$ would grow exponentially, as follows:

$$\mathcal{R}(x,t) = \Delta\mathcal{R}_0 \exp\left[-\gamma\int_0^t \mathrm{d}t'\partial_x h(x,t')\right] \tag{6a}$$

So long as the local slope does not vary too much in space or time, this can be replaced by

$$\mathcal{R}(x,t) \simeq \Delta\mathcal{R}_0 \exp(\gamma S_0 t) \tag{6b}$$

If we now combine these two competing effects, $\mathcal{R}(x,t)$ will either grow or decrease exponentially, according to the relative magnitudes of γS_0 and $v^2/4\mathcal{D}$. If $S_0 > S_d \simeq v^2/4\gamma\mathcal{D}$, rolling grains are generated by dislodgement faster than they are convected downhill – this leads to a catastrophic avalanche, discussed further below. If on the other hand $S_0 < S_d$, the small perturbation is swiftly convected away, leaving the uphill profile in a new quiescent

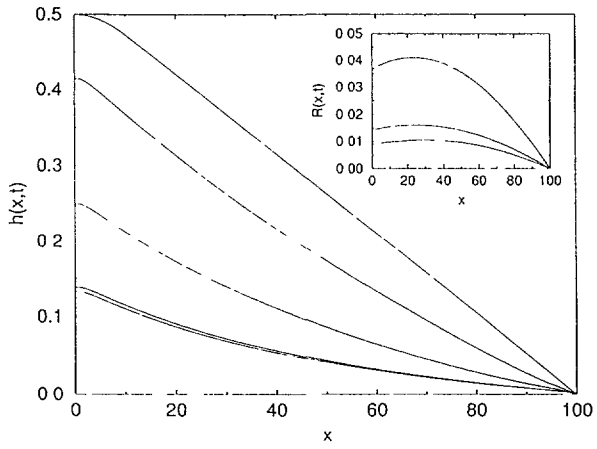

Fig. 4. — Height $h(x,t)$ at different times $t = 1600,\ 2400,\ 4000,\ 5600, 8000$, starting at $t = 0$ (upper curve) from a slope below the spinodal limit $S_0 < S_d$, perturbed from the bottom ($x = L$). The values of the parameters are: $v = 0.1$, $\mathcal{D} = 10$, $\gamma = 1$, $\kappa = 1$. Note that the profile relaxes to a new metastable configuration: the two last curves ($t = 5600$ and 8000) are indistinguishable. Inset: evolution of the rolling grain density as a function of time for the same initial conditions.

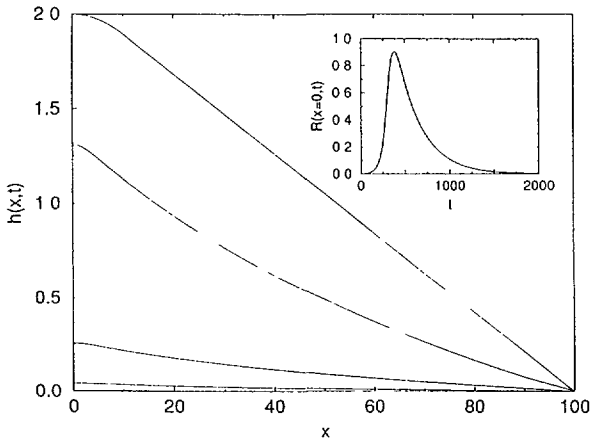

Fig. 5. — Height $h(x,t)$ at different times $t = 300,\ 400,\ 500,\ 700$, but starting at $t = 0$ (upper curve) from a slope *steeper* than the spinodal limit: $S_0 > S_d$, and again perturbed from the bottom ($x = L$). The profile now relaxes to the nominal stable slope S_c (= 0 here): the last curve, corresponding to $t = 700$, has collapsed on the x-axis. Same parameters as in figure 4. Inset: evolution of the rolling grain density *at the upper edge* as a function of time for the same initial conditions.

state. Hence we predict the existence of a sharp critical angle, different from the static angle of repose, above which the profile is unstable to small perturbations. In analogy with the physics of first order transitions, we call this a 'spinodal' angle.

We have confirmed this prediction by numerically solving our equations. The results are displayed in figures 4 to 6. In figures 4 and 5, we show the height profile at different times,

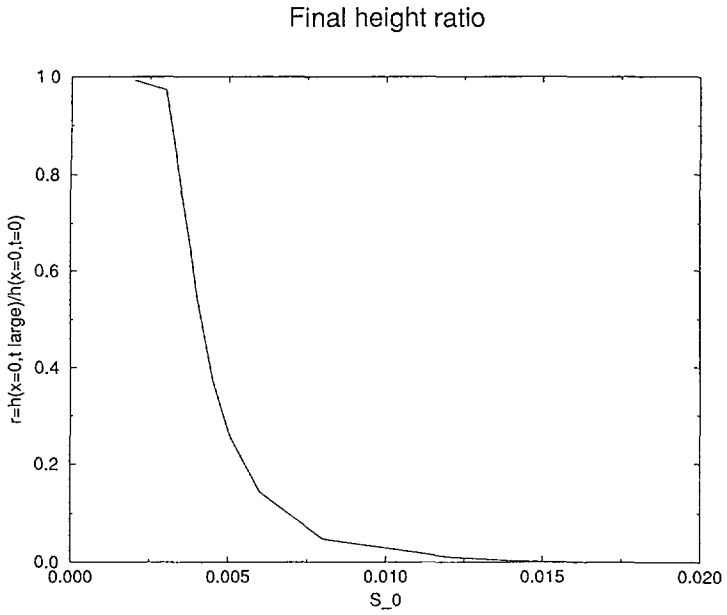

Fig. 6. — Ratio r of the final height $h(x = 0, t = \infty)$ to the initial height $h(x = 0, t = 0)$ as a function of the initial slope S_0. Note that there is a region $S_i < S_0 < S_d$ within which r is neither zero nor one.

both for $S_0 < S_d$, for which the profile relaxes to a new metastable configuration (Fig. 4), and for $S_0 > S_d$, for which the profile relaxes completely to $\dot{h}(x,t) \equiv 0$ (Fig. 5). The perturbation in each case is made at the lower edge of the pile. The inset of figure 4 shows the corresponding profile of $\mathcal{R}(x,t)$, while the inset of figure 5 shows the rolling grain density at the upper edge, $x = 0$ as a function of time. As expected from equation (7) below, $\mathcal{R}(0,t)$ reaches a maximum at a non-zero value of t. Figure 6 shows the ratio of the final height to the initial height at the upper edge, $r = h(0,\infty)/h(0,0)$, as a function of the initial slope S_0. Interestingly, this plot shows evidence for an intermediate range of the initial slope, in which the surface evolves to a final state with r significantly smaller than 1, but still non-zero. (We have found numerically that r is quite insensitive to the initial noise - although the time needed to reach the final value of r grows when $\Delta\mathcal{R}_0 \longrightarrow 0$: see below). $0 < r < 1$ is found when $S_i < S_0 < S_d$, where we estimate, from these data, $S_i \simeq 3v^2/\mathcal{D}\gamma$ and $S_d \simeq (10-20)v^2/\mathcal{D}\gamma$. For $S > S_d$, as argued previously, the relaxation of the surface is complete, and the final state is at the angle of repose $S_c = 0$. The numerical value of S_d is somewhat larger than our naive estimate; this is not surprising since, in approximating equation (6) by $\mathcal{R} = \Delta\mathcal{R}_0 \exp(\gamma S_0 t)$ we ignored the fact that the mean slope itself decays with time.

The difference between S_c (zero, by our convention) and S_d characterizes the role of hysteresis in our model sandpile. In this context, $S_d - S_c$ is known as the Bagnold angle [1, 25]. In our approach, the Bagnold angle is related to physical parameters describing the dynamics of the profile: the dislodging rate γ, the convection velocity of the grains v and, crucially, the diffusion constant $\mathcal{D}$. If $\mathcal{D}$ was equal to zero, there would be no limiting angle of metastability ($S_d \to \infty$) essentially because $\mathcal{R}$ perturbations could not influence anything happening in the uphill direction from where they started. Convection of $\mathcal{R}$ would immediately remove any localized perturbation in the rolling grain density, preventing the feedback mechanism that leads

to instability. As mentioned previously, the diffusion term in equation (2) includes the effects of dislodgement by grains at neighbouring spatial positions (see Sect. 1.3 (iv)), and therefore in practice $\mathcal{D}$ could be a strong function of the background slope S_0. At the level of the above arguments, however, this makes little difference: S_d is given by the root of $S_d \simeq v^2/4\gamma\mathcal{D}(S_d)$ where $\mathcal{D}(S_0)$ represents the slope-dependent effective diffusivity.

Of course (as mentioned in Sect. 1.2) if a static sandpile were tilted through a large enough angle, some grains could cease to be supported by those below, and start rolling. The angle at which this occurs is, in fact, a more conventional interpretation of the Bagnold angle [25], which therefore depends on the local 'roughness' of the profile (see also [16]). In our picture, such an explicit mechanical instability is not necessary for the global structure to be unstable (though it could indeed provide the source for perturbations in $\mathcal{R}$). Nor is it sufficient, since for $S_0 < S_d$ the surface does not relax completely even if some isolated grains do start rolling. Therefore our 'spinodal' interpretation of the Bagnold angle is quite distinct from the usual, mechanical one. Our hysteresis mechanism also differs from that proposed by Jaeger *et al.* [12], which is based on a discussion of the nonmonotonic friction-velocity curve for an individual rolling grain.

The above arguments concerned the effect of a small rolling grain pulse on surface structure *uphill* of the perturbation. It is natural to ask the effect on surface structure on the downhill side – for example, what happens if rolling grains are added to the *upper edge* of a static pile tilted through an angle S_0 beyond the angle of repose. For $S_0 > S_d$, the entire surface again relaxes to zero slope as before, but for intermediate angles the behaviour is more subtle. The perturbation $\Delta\mathcal{R}_0$ of course rolls down the pile, dislodging further grains as it travels. As this pulse passes through the neighborhood of some point x, its integrated effect on the relaxation of $h(x)$ remains finite (for the reasons discussed above, just as if the pulse were initiated at x in the first place). However, the amplitude of the pulse increases (exponentially) with time as it dislodges more and more grains. Therefore, for points far enough downhill from the initial perturbation, the relaxation effect is large and the local slope will relax to values very close to the angle of repose. However, as the perturbation becomes smaller one has to look further and further downhill to see this effect. In fact, since the pulse of rolling grains increases exponentially, the characteristic distance, beyond which nearly complete relaxation occurs, increases as $\simeq \frac{V}{\gamma}\log((S_d - S_0)V/\gamma\Delta\mathcal{R}_0)$.

2.3 THE TIME-SCALE FOR SURFACE RENEWAL. — For $S_0 > S_d$, we expect the initial profile to relax to the truly stable profile $\partial_x h = 0$ after a certain renewal time, or 'flushing time' T which we now estimate. Suppose as before that the initial perturbation is created at the lower edge of the sandpile, $x = L$, where $h(L,t) = 0$ (see Fig. 3). At $x = 0$, we imagine that there is a wall against which the sandpile is leaning. Initially, $h(0,0) = S_0 L$; for definiteness, we define the flushing time T as the half-time for the height of the upper edge of the pile: $h(0,T) = h(0,0)/2$. As a rough estimate, we shall again neglect the time dependence of the mean slope in the evolution equation for $\mathcal{R}$, treating this as a constant, S_0.

Following our previous arguments concerning the competition of convection with dislodgement, we find from equation (2) that the rolling grain density at $x = 0$ and time t is approximated by:

$$\mathcal{R}(0,t) = \frac{\Delta\mathcal{R}_0}{\sqrt{4\pi\mathcal{D}t}} \exp\left[\gamma S_0 t - (L + vt)^2/4\mathcal{D}t\right] \tag{7}$$

On the other hand, from equation (4), one gets $\dot{h} \simeq -\gamma\mathcal{R}S_0$. We can therefore define a certain relaxation time $t^*(\mathcal{R})$ by the equation $h(0,t^*) \simeq h(0,0)/2$; this is easily found to obey $t^*(\mathcal{R}) \simeq L/\gamma\mathcal{R}$. Accounting for the fact that $\mathcal{R}$ is actually time dependent, we estimate the

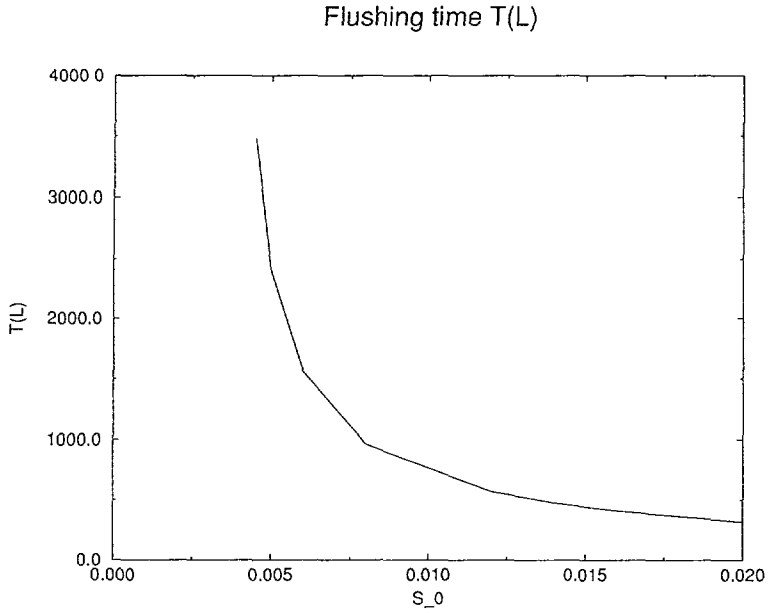

Fig. 7. — 'Flushing time' $T(L)$ as a function of the initial slope S_0 for a Péclet number equal to one. As expected, T becomes small as the 'driving force' S_0 increases, and diverges when $S_0 \longrightarrow S_d$.

flushing time T by the following self-consistency condition:

$$T \simeq t^*(\mathcal{R}) \simeq \frac{L}{\gamma \mathcal{R}(0,T)} \tag{8}$$

with $\mathcal{R}(0,T)$ given by equation (7).

The solution of equation (8) depends on a quantity $\mathrm{Pe} = vL/\mathcal{D}$, which we define by analogy with the usual Péclet number in fluid mechanics. If this is large enough, $\mathrm{Pe} \gg \ell \equiv \log[\gamma T(L) \Delta \mathcal{R}_0 / L]$, one finds that ($\delta \equiv S_0 - S_d$):

$$T(L) \simeq \begin{cases} vL/\gamma \mathcal{D}\delta & \text{for } 0 < \delta \ll S_d \\ L/\sqrt{\gamma \mathcal{D}\delta} & \text{for } \delta \gg S_d \end{cases} \tag{9a}$$

which, to first order, does not depend on the noise level $\Delta \mathcal{R}_0$. For small Pe, one finds:

$$T(L) \simeq \begin{cases} 2\ell/\gamma\delta & \text{for } 0 < \delta \ll 2\mathcal{D}\ell^2/\gamma L^2 \\ L/\sqrt{\gamma \mathcal{D} S_0} & \text{for } S_0 - S_d \gg 2\mathcal{D}\ell^2/\gamma L^2 \end{cases} \tag{9b}$$

(Note that the result for large S_0 is the same for both large and small Pe.) Hence the flushing time decreases with the initial slope S_0 (i.e. the driving force δ) as one might expect.

We now compare these predictions with numerical data. Figure 7 shows T as a function of the initial slope S_0, for $L = 100, \mathcal{D} = 10$ and $v = 0.1$. This corresponds to $\mathrm{Pe} = 1$ which is near the crossover between equations (9a) and (9b). For initial slopes such that $\delta = S_0 - S_d \simeq S_d$, one finds from equation (9a) $T(L) \simeq L/v \simeq 1000$, which is indeed the order of magnitude of the flushing times shown in figure 7; moreoever the flushing time shows a divergence for $S_0 \longrightarrow S_d$ and a decreasing trend for large S_0, in good agreement with equations (9).

2.4 THE ROTATING DRUM. — The above discussion can be used to analyse the 'rotating drum' experiment reported in reference [4], in which a cylinder, partially filled with grains, is rotated around its (horizontal) axis with an angular frequency ω. We shall assume large Pe; this is justified below. If ω is very small, one expects the slope S of the surface of the sand to build up gradually, according to $S(t) = \omega t$, until the spinodal angle S_d is reached at which point a landslide occurs. We presume the mechanics of the drum is imperfect enough to provide the perturbation $\Delta\mathcal{R}_0$ needed to trigger the sandpile instability at S_d. (Amusingly, if the noise level is *too small*, the instability will eventually occur for an angle $S_0 \geq S_d$ - totally irreproducible since it relies on uncontrolled rare events. This might explain why there is an irreducible uncertainty on the determination of S_d, even for very clean experiments [26])

However, it takes a finite avalanche duration $T(L,\omega)$ for the slope to relax after S_d is reached. Defining $t^* = S_d/\omega + T(L,\omega)$, and replacing S_0 by ωt in equation (7), we find that t^* obeys the following equation:

$$4\gamma\mathcal{D}t^{*3} - v^2t^{*2} - (2vL + 4\ell\mathcal{D})t^* - L^2 = 0$$

from which one deduces that (ignoring numerical prefactors) $T(L,\omega) \simeq L/v$ for Pe $\gg 1$ and $T(L,\omega) \simeq \ell\mathcal{D}/v^2$ for Pe $\ll 1$. Notice that $T(L,\omega)$ is in fact independent of ω in both regimes (though different from $T(L)$ for a sudden tilt, as calculated above). Our description is valid *provided the time between avalanches is large compared to the duration of the avalanches themselves*, i.e. $T(L,\omega) \ll S_d/\omega$. In the opposite limit, avalanches overlap strongly: this corresponds to a continuous flow regime, as described in reference [7]. The characteristic angular frequency at which the crossover from isolated avalanches to continuous flow is therefore defined as: $S_d/\omega^* \simeq T(L,\omega^*)$.

This scenario of regular avalanches between two limiting slopes, reminiscent of a first order phase transition [11], emerges naturally from our model and concurs qualitatively with the experimental findings of reference [4]. Interestingly, both the time between successive avalanches S_d/ω and their duration $T(L,\omega)$ were measured in the experiments of Jaeger *et al.*. The values reported in [4] are: $L = 0.1$ m, $\omega = 10^{-3}$ s^{-1}, $T(L,\omega) \simeq 1$ s and $S_d \simeq 5 \times 10^{-2}$ Writing $S_d = Av^2/\gamma\mathcal{D}$, where A is a numerical constant of order 1, we obtain the following parameter estimates: (*i*) By assuming Pe $\gg 1$, one obtains $v \simeq 0.1$ m/s and thus $\gamma\mathcal{D} \simeq A/5$. Consistency of Pe $\gg 1$ then imposes that $\gamma \gg 20A$ s^{-1} Note that a value $\gamma = 100$ s^{-1} corresponds to a lifetime of a rolling grain before sticking, on a surface inclined at 1° below the critical angle, of about 1 s. (*ii*) If instead we assume Pe $\ll 1$, then we deduce $\gamma \simeq A\ell \times 10^2$ s^{-1} and $v^2/\mathcal{D} \simeq 5\ell$. Consistency of Pe $\ll 1$ then imposes that $v \gg 0.5\ell$ m/s.

These estimates do not, unfortunately, allow us to decide the magnitude of Pe without further information concerning (say) v or γ. The crossover value ω^* dividing isolated avalanches from continuous flow can however be predicted, based on our finding that $T(L,\omega)$ is frequency independent, whatever Pe. We obtain $\omega^* \simeq 5 \times 10^{-2}$ s^{-1}, or 0.5 r.p.m, which compares very well with the value quoted by Rajchenbach [7, 27] for a system of glass beads with similar diameter to those used by Jaeger *et al.* [4] (0.25-0.5 r.p.m).

2.5 A SANDPILE WITH STEADY POINT SOURCE. — In all the cases examined numerically, the presence of a steady source of grains relaxes an initially unstable sandpile ($S_0 > S_c$) completely, i.e to S_c, regardless of the value of the initial slope S_0. In the case of a pulse of incident grains, the question of whether enough 'dislodged' grains are generated locally to initiate the relaxation process, before the 'dislodging' grains are convected away, is crucial to the existence of the dynamical angle S_d. However, in the present instance dislodging grains are always present, hence relaxation is always complete.

3. Surface evolution in the presence of noise.

In this section we focus on another aspect of the sandpile problem, of obvious interest to the statistical mechanics community [20, 18, 14, 21, 19], though arguably more remote from the practical world of real sandpiles. We study the long time, large length-scale properties of our equations in the presence of a random noise source. Two sources of noise are considered: noise in the initial condition (initial roughness) which then evolves in time, and spatiotemporal noise, such as is introduced by an incident flux or random "rain" of deposited particles.

3.1 RANDOM INITIAL CONDITION. — We have numerically integrated equations (2-4), using a standard finite difference scheme [28], with a mesh size a (which we associate with the grain size). The simplest case to consider is that of noise in the initial conditions. We start from an initially random surface $h(x,t)$, with an initially constant rolling grain density $\mathcal{R}_0$. The background slope S_c has, as usual, been subtracted so that $h(x,0)$ has mean zero; we take the initial state to have a gaussian white noise spectrum with a small mean-square amplitude h_0^2. We have obtained statistics for the height deviations at long times for large enough samples.

Our data (not shown) is consistent with the following analytical predictions: $\langle \dot{h}(x,t)^2 \rangle \sim t^{-1/2}$ and $\langle \partial_x h^2 \rangle \sim t^{-3/2}$. These exponents can be simply derived by expanding the governing equations (2-4) in small deviations from a uniform rolling grain density $\mathcal{R} = \mathcal{R}_0 + \delta\mathcal{R}$, and solving the problem to lowest order in h and $\delta\mathcal{R}$. Equations (3) and (4) then reduce to the following linearized equations:

$$\delta\dot{\mathcal{R}} = -v\partial_x \delta\mathcal{R} + \mathcal{D}\partial_x^2 \delta\mathcal{R} - \dot{h} \tag{10a}$$

$$\dot{h} = \mathcal{R}_0[\gamma\partial_x h + \kappa\partial_x^2 h] \tag{10b}$$

The second of these is a straightforward convection diffusion equation for h (with convection in the uphill direction, as discussed previously). The convection term has only a trivial effect since the random initial condition is already homogeneous. The diffusive term smears out the height fluctuations within a time dependent diffusion length $\xi(t) \simeq \sqrt{\mathcal{R}_0 \kappa t}$. The typical height fluctuation can be estimated simply by averaging $\xi(t)/a$ samples from the initial distribution (corresponding to the initial heights at all mesh points within the diffusion length). Since these have mean zero and rms deviation h_0, one has $h \simeq h_0/\sqrt{\xi(t)} \sim t^{-1/4}$. A similar argument gives $\partial_x h \simeq h/\xi \sim t^{-3/4}$. It is gratifying that our numerical data may be rationalized so simply (and in fact this can be done much more rigorously [29]). Since the initial roughness decays in time, it is perhaps not surprising that the linearized model becomes valid at long times. The situation is less obvious with a steady noise term, as we now consider.

3.2 RANDOM INCIDENT FLUX. — We have also investigated numerically the role of a random rain of soft grains governed by an incident flux $\eta(x,t)$ added to the h equation (Eq. (4)). For this study we did *not* include a KPZ term, $(\partial_x h)^2$; the role of such a term is discussed in section 3.4 below. For $\eta(x,t)$ we chose a white noise such that $\langle \eta(x,t)\eta(x',t') \rangle_c = 2\sigma \times \delta(x-x')\delta(t-t')$, where $\langle\rangle_c$ denotes a cumulant. Thus the mean incident flux, which leads to a steady upward translation of the surface, has been subtracted.

One interesting outcome of our numerical work is that, in order reach a well-defined scaling regime, the sandpile must be given a mean slope S_η slightly less than S_c (i.e. the slope must be flatter than critical). If a slope S_c is used, the rolling grain density increases exponentially in time. This crosses over to exponential decay at slopes less than S_η; only for $S = S_\eta$ is a scaling condition obtained. In practise, one can dynamically tune to the critical slope S_η by

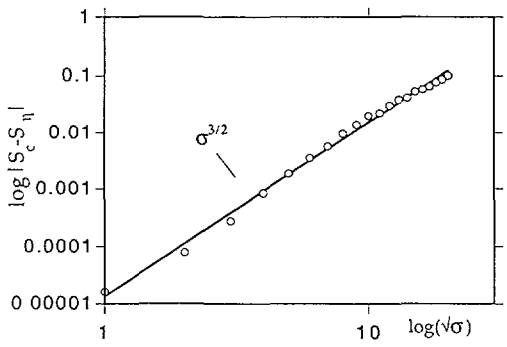

Fig. 8. — Noise induced dynamical slope (minus the nominal stability slope S_c) as a function of the noise level, with a power law fit with exponent 3/2. The noisier the flux used to generate the pile, the flatter the resulting slope.

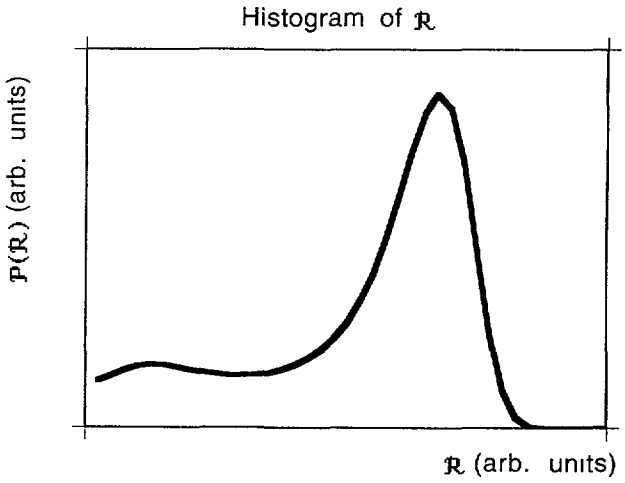

Fig. 9. — Histogram of the local rolling grain density in the presence of a random rain of particles: we have plotted $\log P(\mathcal{R})$ as a function of $\mathcal{R}$, which would be a parabola for Gaussian fluctuations, as observed when the input noise is small. Larger noise induce 'intermittency' (see Fig. 10), with a peak developing at small values of $\mathcal{R}$.

insisting that the total number of rolling grains in the system remains constant. The behaviour of our noise-induced dynamical slope $S_\eta(\sigma)$ is presented in figure 8, where we show $S_c - S_\eta$ as a function of the noise level σ. Unexpectedly, our data can be fitted by a nontrivial power-law: $S_c - S_\eta = A(v)\sigma^\beta$, with an exponent $\beta \simeq 3/2$, and an amplitude $A(v)$ which is a decreasing function of the rolling grain velocity v. Physically, this means that the larger the noise, the flatter the pile which is constructed - the true angle of repose S_c is only reached in 'careful' conditions ($\sigma = 0$). The static structure factor, $\langle h(k,t)h(-k,t)\rangle$, and the time evolution of $\langle \dot{h}(x,t)^2 \rangle$ and $\langle \delta\mathcal{R}(x,t)^2 \rangle$ are consistent with those predicted by the linearized theory in the

presence of noise: we find $\langle h(k,t)h(-k,t)\rangle \sim k^{-2}$, with both $\langle h^2\rangle$ and $\langle \delta\mathcal{R}^2\rangle$ scaling as $t^{1/2}$. (The latter result for $\mathcal{R}$ fluctuations of course does not contradict the fact that the total number of rolling grains remains constant in time for $S = S_\eta$.) The results for the height variable correspond to the Edwards Wilkinson model [29] which is obtained by adding the noise term η to equation (10b); since the noise term is translationally invariant, the convective term in that equation again plays no role. The surface is asymptotically rough, in contrast to the asympototic flatness predicted by the Hwa-Kardar model (Eq. (1)) [14].

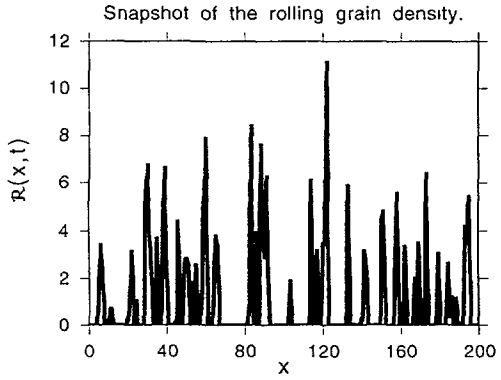

Fig. 10. — Snapshot of the rolling grain density $\mathcal{R}(x,t)$ at a given instant of time, showing quiescent regions coexisting with 'avalanches'.

Although our model follows the scaling exponents of the linear theory, the probability distribution of the local rolling grain density $\mathcal{P}(\mathcal{R})$ is highly nontrivial. For small values of the noise, the numerics show a nearly Gaussian distribution of fluctuations about a well-defined mean; however, for larger noise amplitudes the distribution becomes skewed and exhibits a significant tail for small values of $\mathcal{R}$, corresponding to the presence of locally 'frozen' regions (Fig 9). A plot of the spatial variation of $\mathcal{R}$ at a given instant of time is shown in figure 10. It is clear that for large-amplitude disorder, the rolling grain density shows strong intermittency, with many quiescent zones separating irregular bursts. We have also investigated the time autocorrelation of the flux (or "avalanche density") $v\mathcal{R}$. The linearized theory predicts that the autocorrelation function $v^2\langle \delta\mathcal{R}(x,t)\delta\mathcal{R}(x,0)\rangle$ decays with time as $\exp[-v^2t/\mathcal{D}]$, again consistent with our numerical results. The absence of long time correlations arises because the non-zero convective velocity v sweeps away the fluctuations as they are formed. This prediction is at variance with other theoretical approaches [3, 14], where broad spectrum $(1/f)$ noise was proposed for the flux down the slope.

3.3 PERTURBATION THEORY FOR WEAK NONLINEARITY. — We now set up a formal perturbation expansion about the linearized equations (these are Eq. (10a), and Eq. (10b) with the noise term η added on the right) to study the nonlinearity arising from a random incident flux of soft grains. We will see that this perturbation theory is well-behaved, which indicates that the power-law exponents predicted from the linearized model should remain valid, although the nonlinearity will alter the amplitudes of the correlation functions.

Writing $\mathcal{R} = \mathcal{R}_0 + \delta\mathcal{R}$ and taking the Fourier transform of equations (2-4), we obtain the

following equations (at wavevector k and frequency ω):

$$(i\omega + ivk + \mathcal{D}k^2)\delta\mathcal{R}(k,\omega) = -iv_h kh(k,\omega) - i\gamma \int \frac{dq}{2\pi}\frac{d\Omega}{2\pi}\, qh(q,\Omega)\delta\mathcal{R}(k-q,\omega-\Omega) \qquad (11a)$$

$$(i\omega - iv_h k + \kappa\mathcal{R}_0 k^2)h(k,\omega) = \eta(k,\omega) + i\gamma \int \frac{dq}{2\pi}\frac{d\Omega}{2\pi}\, qh(q,\Omega)\delta\mathcal{R}(k-q,\omega-\Omega) \qquad (11b)$$

Where $v_h = \gamma\mathcal{R}_0 > 0$ is the magnitude of the uphill convection velocity of surface features (introduced in Sect. 2). We have neglected terms corresponding to $\kappa\delta\mathcal{R}\partial_x^2 h$ in Γ, since these involve higher powers of k than the parts retained, and will thus be unimportant for the interesting limit of small wavevector and frequency.

Expanding equations (11a) and (11b) in powers of γ (with v_h held constant) and eliminating $\delta\mathcal{R}(k,\omega)$ from equation (11b), one finds the following perturbative expansion for $h(k,\omega)$:

$$h(k,\omega) = G_0(k,\omega)\eta(k,\omega) + \gamma v_h G_0(k,\omega)\int \frac{dq}{2\pi} q(k-q)h(q,\omega_q)h(k-q,\omega-\omega_q)$$

$$+i\gamma^2 v_h G_0(k,\omega)\int \frac{dq}{2\pi}\frac{dp}{2\pi} q(k-p)(p-q)h(q,\omega_q)h(k-p,\omega-\omega_p)h(p-q,\omega_{p-q})$$

$$+O(\gamma^3) \qquad (12)$$

where $G_0(k,\omega) \equiv (i\omega - iv_h k + \kappa\mathcal{R}_0 k^2)^{-1}$ and $\omega_q \equiv -vq + i\mathcal{D}q^2$.

Having eliminated the rolling grains, we are left in equation (12) with an evolution model for h, including nonlinear terms, whose effect can be studied by following standard procedures (see e.g. [17, 20, 18]). Formally one recasts the dynamical equation in terms of perturbative expansions for the response function $G(k,\omega) \equiv \langle \frac{\partial h(k,\omega)}{\partial \eta(k,\omega)} \rangle$ and for the correlation function $\langle h(k,\omega)h(-k,-\omega)\rangle$. These consist of the bare values (as given by linear theory) plus correction terms in the form of integrals. For example, to order γ^2, $G(k,\omega)$ reads:

$$G(k,\omega) = G_0(k,\omega) - 8\gamma^2 v_h^2 \sigma G_0^2(k,\omega)k\int \frac{dq}{2\pi} q^2(k-q)G_0(q,\omega_q)G_0(-q,\omega_{-q})G_0(k-q,\omega-\omega_q)$$

$$+6i\gamma^2 v_h \sigma G_0^2(k,\omega)k\int \frac{dq}{2\pi} q^2 G_0(q,\omega_q)G_0(-q,\omega_{-q}) \qquad (12')$$

It is straightforward to check that these integral corrections are all convergent. In the language of critical phenomena, the nonlinearity is therefore "irrelevant". This means that the perturbation expansion should, for weak nonlinearity, lead only to finite shifts in the effective parameter values (such as the uphill convection velocity, $\gamma\mathcal{R}_0$, or the effective surface tension, $\kappa\mathcal{R}_0$) from those of the linearized theory. For example, the lowest correction to the uphill convection velocity for height fluctuations is:

$$[v_h]_{\text{eff}} - v_h = +\frac{4\gamma^2(3v - v_h)v_h\sigma}{(v_h+v)^3 a} \qquad (13)$$

Thus the combined action of noise and non-linearity is to speed up or to slow down the uphill convection of surface features, depending on the sign of $3v - v_h$ [30].

Our perturbation theory will presumably start to break down when the nonlinearity is strong enough. However, there is no sign of such complications in our numerical results given earlier; in practice the scaling behaviour, $\langle h(k,t)h(-k,t)\rangle \sim k^{-2}$, and $\langle h^2\rangle$, $\langle \delta\mathcal{R}^2\rangle \sim t^{1/2}$, remains that of the linearized model. As is the case for analagous problems involving critical phenomena under flow [31], it appears that the steady convection of surface features suppresses the buildup of fluctuations, preventing the occurrence of large nonlinear correction terms: note that $[v_h]_{\text{eff}}$ diverges when the relative velocity $v_h + v$ goes to zero.

3.4 OTHER TYPES OF NONLINEARITY. — Some other forms of nonlinearity were discussed earlier (Sect. 1.3), points (v-viii)) which are missing from our treatment so far.

Various contributions could arise from including a dependence of the velocity of the rolling grains v either on the local slope (as one might expect) or on the density of rolling grains (which would represent a hindering effect). It is straightforward to check that for noisy deposition these nonlinear terms are also "irrelevant", i.e., they lead to convergent integrals in the perturbation theory; the same applies to similar dependences of the diffusion constant $\mathcal{D}$.

The same is *not* true however of the KPZ nonlinearity, as discussed in point (vii) of section 1.3, which is intended to describe the dependence of the mean incident flux of incoming particles or of γ on the local slope of the surface. The KPZ equation [20], which describes random deposition onto horizontal surfaces, is obtained by adding a term $\lambda(\partial_x h)^2$ to the right of equation (10b), and setting $v_h = 0$:

$$\dot{h} = \nu \partial_x^2 h + \lambda(\partial_x h)^2 + \eta$$

where we have identified the bare "surface tension" as $\mathcal{R}_0 \kappa = \nu$. In the present context, for nonzero incident mean flux, we should analogously add a term $\lambda(\partial_x h)^2$ to equation (4). This gives the following contribution to the right hand side of equation (12):

$$-\lambda G_0(k,\omega) \int\int \frac{\mathrm{d}q}{2\pi} \, [q(k-q)] \; h(q,\Omega) h(k-q, \omega - \Omega) \tag{14}$$

Perturbation theory to second order in λ shows that this term is relevant (in space dimensions $d \leq 2$): the divergence induced is the one encountered for the usual KPZ equation [20, 18]. This term strongly affects the effective surface tension, which becomes k dependent. For two dimensions (as here) the KPZ model predicts that for large times, $\langle h(k,t) h(-k,t) \rangle \sim k^{-2}$, and $\langle [h(x,t) - h(x,0)]^2 \rangle \sim t^{2/3}$ These scaling form are expected to hold in the presence of all the others, irrelevant, non linearities which we have discussed. The presence of a KPZ term however leads to some subtlety involving the conservation condition on grains, which imposes that $\dot{h} + \dot{\mathcal{R}} = \partial_x j + \eta$ where j is a suitably defined current, and η the incident flux. For the model just considered, this reads instead $\dot{h} + \dot{\mathcal{R}} = \partial_x j + \lambda(\partial_x h)^2 + \eta$. Clearly, the conservation law is restored by adding a counter-term $-\lambda(\partial_x h)^2$ to the equation for $\mathcal{R}$, equation (2). However, it is arguable that this conservation law should not hold in general in granular media, where the local density can change e.g. under stress. But in fact, such a KPZ term in the $\mathcal{R}(x,t)$ equation is anyway expected to appear from the nonlinear dependence of Γ on $\partial_x h$ as considered in section 1.3 (viii). For completeness, therefore, we have checked the effect of adding a counterterm to the $\mathcal{R}(x,t)$ equation as just described. This yields in equation (12) a further contribution of a rather different form,

$$-i\gamma\tilde{\lambda} G_0(k,\omega) \int \frac{\mathrm{d}q}{2\pi} \frac{\mathrm{d}p}{2\pi} \frac{d\Omega}{2\pi} \, [q(k-p)(p-q)] \; h(q,\Omega) h(k-p, \omega - \omega_p) h(p-q, \omega_p - \Omega) \tag{15}$$

The term appears only to affect the uphill velocity $[v_h]_{\text{eff}}$ which will also become k dependent, while giving a *finite* correction to the surface tension $\mathcal{R}_0 \kappa$. Although we have not analysed this in detail, it seems likely that the height exponents are not affected by this 'Doppler like' perturbation, and remain at their standard KPZ values. This trend is confirmed by a numerical simulation of the governing equations with both terms present: see figures 11 and 12.

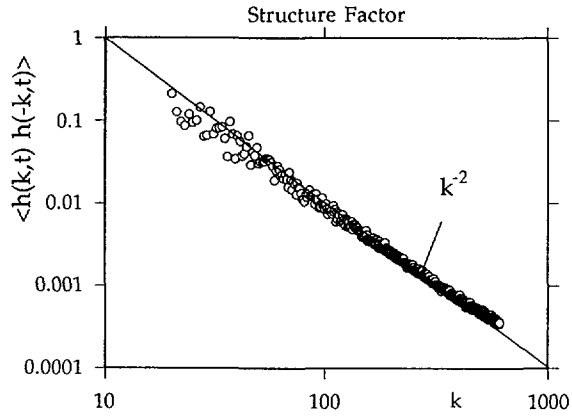

Fig. 11. — Height statistics $< h(k,t)h(-k,t) >$ as a function of the wave number k when a 'KPZ' term is added to the rolling grain density equation equation. The KPZ behaviour $< h(k,t)h(-k,t) > \simeq k^{-2}$ is maintained.

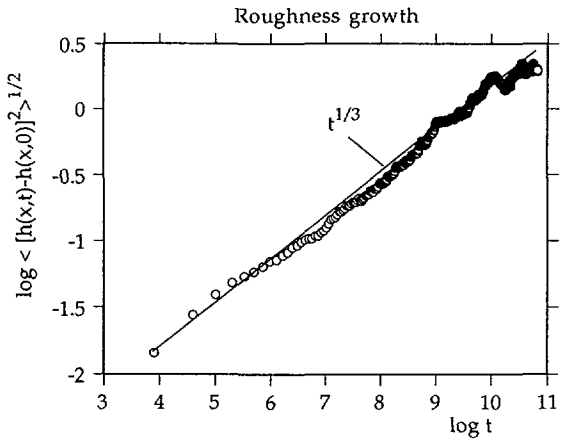

Fig. 12. — Growth of the height fluctuations $< [h(x,t) - h(x,t=0)]^2 >^{1/2}$ as a function of time, in the presence of a KPZ term in the rolling grain density equation. Again, the KPZ exponent $t^{1/3}$ is observed.

3.5 A SANDPILE WITH NOISY POINT SOURCE. — We have finally investigated in a qualitative manner the effect of a noisy point source at the top of the pile. The main question is to know how the non-linear 'black-box' separating the input point at the top from the exit point at the bottom transforms the statistics of the input noise. In particular, one could wonder if a short range correlated input noise could generate a 'colored' noise in the exit flux; this would reflect a nontrivial (e.g., power law) avalanche size distribution. Figure 13 shows on the same graph the input and exit flux as a function of time; revealing indeed an increase in correlation time. A more systematic statistical analysis of this important question (in view of the number of recent discussions related to the avalanche size distribution) is however needed, and we defer it for future work.

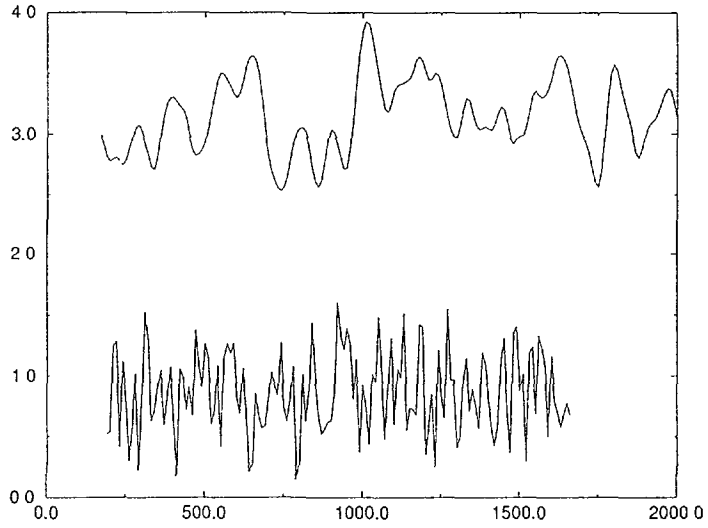

Fig. 13. — Exit flux as a function of time (top curve), for a random input flux at the top of the pile (bottom curve), represented on the same plot.

4. Derivation from a microscopic model.

In this section we show how our continuum equations (2, 4) can be obtained from a discrete microscopic model involving the stochastic dynamics of individual grains. In fact it was the study of this model which initiated the present work; logically, therefore, this section might have been placed first. We have deferred our discussion until now because the continuum equations, once formulated, are rather easier to use, especially in analytical work, once our choice of a simplified, bilinear interconversion kernel (Eq. (3)) has been made.

The microscopic model discussed below remains phenomenological, insofar as it contains various parameters which we do not attempt to predict. Nonetheless, it allows us to complete a conceptual bridge between the local microphysics of sandpiles and their observed macroscopic behaviour. We limit attention to the case of "hard" grains, for which any external flux feeds into the population of rolling grains, rather than the immobile ones. This is the opposite case from that considered in section 3; however, the generalization is straightforward.

4.1 SURFACE KINETICS — We consider a discretized two dimensional sandpile, constructed by dropping grains of sand onto a line. This baseline is divided into intervals of length a, which are labelled $i, i+1$ etc., and events (such as grain addition) occur at various times t_α, t_β etc.. Time is also discretized, so motion of grains occurs in discrete hops from one site to another. In what follows, the term "adsorption" means sticking of a mobile grain to the pile at a given site to form an immobile grain. Also, we shall make a distinction between "rolling" grains and "mobile" grains. The latter represent, essentially, those grains capable of rolling at the next time step. The distinction becomes unimportant in the continuum limit, but is a useful bookkeeping device in our discrete model.

We now consider some particular site i at time t_α, denoted hereafter as (i,α) we can write for the corresponding change in the number n of immobile grains:

$$\Delta n_{i\alpha} = \psi_{i\alpha}(F_{i\alpha} + R_{i\alpha}) - L_{i\alpha} \tag{16}$$

where $\psi_{i\alpha}$ is the local sticking probability. Here $F_{i\alpha}$ represents the number of incident grains added to the pile at (i,α) from external sources, whereas $R_{i\alpha}$ is the number of "rolling" grains arriving at (i,α) (grains which have not just been added, but which were previously either added or dislodged at some different site). The quantity $L_{i\alpha}$ represents the number of grains newly dislodged at (i,α).

We now introduce a quantity

$$m_{i\alpha} = (F_{i\alpha} + R_{i\alpha})(1 - \psi_{i\alpha}) + L_{i\alpha} \tag{17}$$

This represents the total number of *mobile* grains at (i,α), namely grains that have arrived from an external source but are not adsorbed $(F(1-\psi))$; rolling grains arrived but not adsorbed $(R(1-\psi))$; and dislodged grains newly produced (L). Finally we define $\chi_{i\alpha,j\beta}$ as the transition probability that a mobile grain at (j,β) moves to (i,α) without making contact with the pile between these two times. In general, this can include local and long range jumps of all kinds reflecting rolling, bouncing *etc.*, though below we will specialize to a simpler form for $\chi_{i\alpha,j\beta}$.

With these definitions, we obtain for the rolling grain density

$$R_{i\alpha} = \sum_{\beta=0}^{\alpha-1} \sum_{j} \chi_{i\alpha,j\beta}\ m_{j,\beta} \tag{18}$$

which means physically that the rolling grains at site i at time t_α consist of all mobile grains, present at sites j and earlier times t_β, that have moved from there directly to (i,α). Equations (16, 17) may be easily rearranged to give

$$\Delta n_{i\alpha} = \left(\frac{\psi_{i\alpha}}{1-\psi_{i\alpha}}\right) m_{i\alpha} - \left(\frac{1}{1-\psi_{i\alpha}}\right) L_{i\alpha} \tag{19}$$

Our results so far are very general. To make use of them, we must make some simplifying assumptions. The first of these concerns the transition probability $\chi_{i\alpha,j\beta}$. For simplicity we assume

$$\chi_{i\alpha,j\beta} = (\frac{1}{2} - \epsilon)\delta_{\alpha-1,\beta}\delta_{i+1,j} + (\frac{1}{2} + \epsilon)\delta_{\alpha-1,\beta}\delta_{i-1,j} \tag{20}$$

with ϵ a parameter. This describes particles that can only transmit to nearest neighbour sites in a single time step. (It thus describes the rolling of grains, but not, in principle, any long-range hops or "bounces".) Unless $\epsilon = 0$, there is a built-in preference for jumping downhill (i.e., increasing i), reflecting the presence of a background slope.

Substituting this form into the defining equation (18) for R gives

$$R_{i\alpha} = (\frac{1}{2} - \epsilon)m_{i+1,\alpha-1} + (\frac{1}{2} + \epsilon)m_{i-1,\alpha-1} \tag{20'}$$

If we now eliminate $L_{i\alpha}$ and $R_{i\alpha}$ from equation (17) using (16) and (20) we obtain

$$m_{i\alpha} - (\frac{1}{2} - \epsilon)m_{i+1,\alpha-1} - (\frac{1}{2} + \epsilon)m_{i-1,\alpha-1} = F_{i\alpha} - \Delta n_{i\alpha} \tag{21}$$

Equations (19) and (21) are a pair of coupled equations, local in time and space, for the evolution of the numer of adsorbed grains, n, the number of mobile grains, m, at neighbouring sites. The external flux is F, whereas the adsorbtion probability ψ and dislodgement rate L for each site remain to be chosen.

4.2 THE CONTINUUM LIMIT. — We now seek the continuum limit for equations (19, 21). We denote the discretization length by a, as previously, and the discrete time interval (jump time) by τ. We must first associate our discrete variables $n, \Delta n, F, \psi, L$ and m (each of which is dimensionless) with a set of (dimensioned) continuum variables. This can be done in several ways, but most straightforwardly by dimensional analysis, with the following results:

$$\begin{aligned} n_{i\alpha} &= h(x,t)/a \quad , \quad \Delta n_{i\alpha} = \dot{h}(x,t)\tau/a \\ F_{i\alpha} &= \phi(x,t)a\tau \quad , \quad L_{i\alpha} = \lambda(x,t)a\tau \\ \psi_{i\alpha} &= p(x,t)\tau \quad ; \quad m_{i\alpha} = m(x,t)a \end{aligned} \tag{22}$$

Here $h(x,t)$ is the height; $\dot{h}$ its time derivative; $\phi(x,t)$ the incident flux (particles arriving per unit time per unit length); $p(x,t)$ the probability per unit time of a mobile particle sticking; $\lambda(x,t)$ the rate of production of rolling particles by dislodgement per unit length and time; and $m(x,t)$ the number of mobile grains per unit length.

Making these substitutions in equation (19), and letting the time increment become small ($\tau \to 0$) at fixed sticking probability p yields

$$\dot{h}(x,t)/a^2 = p(x,t)m(x,t) - \lambda(x,t) \tag{23}$$

This makes sense when one realizes that h/a^2 is the total number of immobile grains per unit length: pm represents the adsorption of mobile grains and λ the loss of immobile grains due to the dislodgement process.

We now apply the same limiting procedure to equation (21). We further assume that the density of mobile grains $m(x,t)$ can be represented as a smooth function of position and time. By expanding on the left of (21) in a double Taylor series, we obtain:

$$\dot{m} + 2\epsilon(a/\tau)\partial_x m - (a^2/2\tau)\partial_x^2 m + O(\tau^2, a^3) = \phi - \dot{h}/a^2 \tag{24}$$

To eliminate the dependence on a, we introduce physical quantities $\mathcal{R} = ma^2$, $\eta = \phi a^2$, and $\Lambda = \lambda a^2$ which remain well-defined in the continuum limit. Thus $\mathcal{R}(x,t)$ is the contribution that mobile grains would make to the height h if suddenly immobilized; $\eta(x,t)$ is the contribution that any incident flux would make to $\dot{h}$ under the same condition; and Λ is the rate of height loss from dislodgement. We also define variables $\mathcal{D} = a^2/2\tau$ and $v = 2\epsilon a/\tau$, which (by taking $\epsilon \sim a$) can both be made to remain finite as $a \to 0$ and $\tau \to 0$.

With these definitions, equations (23, 24) become

$$\dot{h} = p(x,t)\mathcal{R} - \Lambda(x,t) \tag{25a}$$

$$\dot{\mathcal{R}} + v\partial_x \mathcal{R} - \mathcal{D}\partial_x^2 \mathcal{R} = \eta - \dot{h} \tag{25b}$$

These correspond to equations (2) and (4), with a constant velocity v and diffusion constant $\mathcal{D}$. Note that the incident flux term η is added to the $\dot{\mathcal{R}}$ equation. This model therefore represents the physics of "hard" grains, as defined earlier, for which any grain that lands on the pile is initially mobile. The interconversion kernel in the present model is of the form

$$\Gamma = -p(x,t)\mathcal{R}(x,t) + \Lambda(x,t) \tag{26}$$

with p the local sticking probability and Λ the dislodgement rate.

At this point we could make a sequence of physically motivated assumptions, in the framework of the microscopic model, to simplify the form of Γ. However, we have already carried out the corresponding procedure, at the macroscopic level, in section 1.2. The simplified bilinear kernel (Eq. (3)) follows from (26) if we assume (i) that the dislodgement rate Λ is proportional to the density of mobile grains, so that $\Lambda = q(x,t)\mathcal{R}$, and (ii) that the quantity $q(x,t) - p(x,t)$ can be expanded as a Taylor series in $h(x,t)$ and its spatial derivatives. The latter requires that $h(x,t)$ can be treated as smoothly varying. We have not needed to assume this so far in this section, although a corresponding assumption was made earlier for $m(x,t)$ (in deriving Eq. (24) above).

The above considerations lead to a model with a finite diffusion constant $\mathcal{D}$ which arises from the ability of grains to hop uphill. As mentioned in section 1.3 (iv), the diffusion term in equation (2) is intended also to model the fact that dislodgement of a given immobile grain can be initiated by mobile grains, not just at the same site but at neighbouring ones. As discussed there, this would lead to a presumably slope-dependent diffusion constant. To model the case where this process is the dominant form of dispersion, the hopping diffusion $\mathcal{D}$ can be "switched off" by taking a slightly different continuum limit of the discrete picture: if we maintain ϵ finite (e.g., $\epsilon = 1/2$, corresponding to fully directed motion) as $a \to 0$ and $\tau \sim a \to 0$, then $\mathcal{D} = 0$ whereas $v = 2\epsilon a/\tau$, as before Any dislodgement-induced dispersion, of the type just described, would then have to be explicitly included in the kernel Γ.

5. Conclusions

We now summarize the main points of this paper. First, we have established, using general physical arguments, a set of phenomenological equations (2-4) with which to describe the evolution of the sloped surface of a sandpile or similar granular aggregate, close to the angle of repose. These equations differ from earlier analyses in their explicit inclusion of two interacting variables, the local height of the pile and the local density of mobile ("rolling") grains. The latter is subject to a steady downhill convection arising from the background slope. The interconversion of immobile and rolling grains was represented by a simplified bilinear kernel with relatively tractable analytic properties.

Several interesting aspects of sandpile dynamics have been predicted using the model. Firstly (see Sect. 2.1) the downhill convection of rolling grains leads to an uphill convection of surface features. For a steady initial rolling grain density, small features will be convected uniformly, whereas large amplitude features will tend to shock. Secondly (see Sects. 2.2, 2.3) our equations exhibit the physically important property of *metastability* leading to hysteresis effects. A sandpile at the angle of repose will not relax fully when tilted unless a finite threshold (the Bagnold angle) is exceeded. In our model, this corresponds to a 'spinodal' angle beyond which infinitesimal perturbations can lead to relaxation of the pile. This spinodal angle can be expressed in terms of the other parameters entering the model, some of which can be estimated from rotating drum experiments (see Sect. 2.4); qualitative agreement is obtained between our predictions of the avalanche/continuous flow transition and the observed value.

We have also investigated our equations in the presence of various noise terms, focusing on the long time, large length-scale properties. For a random initial condition with no external flux (see Sect. 3.1), the initial roughness decays in time with exponents corresponding to those of the linearized version of the theory. For homogeneous spatiotemporal noise, and in the absence of any KPZ term, our nonlinear equations again display the asymptotic properties of their linearized counterparts; the height fluctuations therefore show Edwards–Wilkinson scaling (see Sects. 3.2, 3.3). The steady downhill convection of grains inhibits the buildup of

fluctuations; the current autocorrelation function decays exponentially in time. If a KPZ term is added, however (appropriate in the presence of a nonzero incident mean flux) it remains relevant despite the convection, and we recover numerically the anomalous exponents of the KPZ model (see Sect. 3.4). According to whether this term is included, the surface dynamics are either diffusive ($\xi(t) \sim t^{1/2}$), or of the KPZ type ($\xi(t) \sim t^{2/3}$). In either case, the sandpile surface is predicted to be rough, i.e., height variations increase with separation. These results differ significantly from those of Hwa and Kardar who predict a flat surface and a correlation length $\xi(t) \sim t$.

Finally, in section 4, we have shown explicitly how to obtain our phenomenological continuum description of rolling and immobile populations, starting from a discretized microscopic model that considers the local motions of individual grains. This helps to clarify the physical approximations we have made, and completes a conceptual link between the microphysics of sandpile surfaces and their macroscopic behaviour.

All the results summarized above are for sandpiles in two-dimensional space (the height is a function of one position variable, and time). As mentioned in the introduction, our equations generalize straightforwardly to higher dimensions. Most of the interesting physical properties that we have predicted carry over, or have obvious analogues, in higher dimensions. Another direction would be to apply similar ideas to surface growth. Assuming that one still has two populations of particles (moving or stuck), one could consider the following equations:

$$\frac{\partial h(\vec{x},t)}{\partial t} = -\Gamma = \lambda_1 \vec{\nabla}\mathcal{R}(\vec{x},t)\cdot\vec{\nabla}h(\vec{x},t) + \lambda_2 \mathcal{R}(\vec{x},t)\nabla^2 h(\vec{x},t) \tag{27a}$$

$$\frac{\partial \mathcal{R}(\vec{x},t)}{\partial t} = \mathcal{D}\nabla^2\mathcal{R}(\vec{x},t) + \Gamma + \eta(\vec{x},t) \tag{27b}$$

as alternatives to the usual KPZ description. We leave the detailed investigation of these extensions open to future study.

Acknowledgements.

One of us (MEC) is grateful to Anita Mehta for several useful discussions on sandpile dynamics. JPB wants to thank E. Clement, J. Duran, P. Evesque and J. Rajchenbach for important comments. Part of this work was supported by the Colloid Technology Programme funded by Unilever, Schlumberger, ICI and the Department of Trade and Industry (UK). After completing this work we learned that Mehta, Needs and Luck have simultaneously developed coupled equations for h and $\mathcal{R}$ variables which share certain features with our own (though differing in other key respects). See [16], (1994)

Appendix.
The solution procedure.

In this appendix we describe a solution method suitable for dealing with the deterministic examples of section 2. The results of section 3 in the presence of 'strong noise' were instead obtained using a standard finite difference time-march scheme. The basic equations (2) and (4) are a pair of second order quasi-linear partial differential equations in the dependent variables $h(x,t)$ and $\mathcal{R}(x,t)$. They may be solved by methods developed for first order equations, by rewriting them in matrix form as,

$$\mathbf{A}(\mathbf{w})\frac{\partial \mathbf{w}}{\partial t} + \mathbf{B}(\mathbf{w})\frac{\partial \mathbf{w}}{\partial x} = \mathbf{C} \tag{A.1}$$

where $\mathbf{w} \equiv (\dot{h}(x,t), \mathcal{R}(x,t))$, $\mathbf{A}$ and $\mathbf{B}$ are matrices whose elements are functions of $\mathbf{w}$. The inhomogeneous term $\mathbf{C}$ is a column vector containing the second order derivatives, along with any external perturbing terms (such as a noisy incident flux η). Equation (13) can be classified as 'hyperbolic' [32, 33], since the characteristic equation

$$\det(\mathbf{B} - \lambda\mathbf{A}) = 0$$

has two real roots, $\lambda_1 = -\gamma\mathcal{R}$ and $\lambda_2 = v$, and there are two linearly independent eigenvectors, $\mathbf{l}_j$, such that

$$\mathbf{l}_j^{\mathrm{T}}(\mathbf{B} - \lambda_j\mathbf{A}) = 0; \qquad j = 1,2 \tag{A.2}$$

As a consequence, there are two characteristic curves along which the basic equations reduce to compatibility conditions. To describe these, we introduce the notation

$$\frac{D_i}{Ds} \equiv \left(\frac{\mathrm{d}t}{\mathrm{d}s}\right)_i \frac{\partial}{\partial t} + \left(\frac{\mathrm{d}x}{\mathrm{d}s}\right)_i \frac{\partial}{\partial x}$$

The first curve can be then written in parametric form as

$$\frac{\mathrm{d}t}{\mathrm{d}s} = 1; \qquad \frac{\mathrm{d}x}{\mathrm{d}s} = -\gamma\mathcal{R} \tag{A.3}$$

along which the following compatibility condition applies:

$$\frac{D_1 h}{Ds} = \kappa\mathcal{R}\partial_x^2 h \tag{A.4}$$

The second curve has the parametric form

$$\frac{\mathrm{d}t}{\mathrm{d}s} = 1; \qquad \frac{\mathrm{d}x}{\mathrm{d}s} = v \tag{A.5}$$

with the compatibility condition

$$\frac{\gamma\mathcal{R}}{(\gamma\mathcal{R}+v)}\frac{D_2 h}{Ds} + \frac{D_2\mathcal{R}}{Ds} = \mathcal{D}\,\partial_x^2\mathcal{R} - \frac{v\kappa\mathcal{R}\partial_x^2 h}{(\gamma\mathcal{R}+v)} + \eta \tag{A.6}$$

The numerical procedure is based on an inverse marching scheme [34], wherein characteristics are drawn backwards from any point $\mathbf{w}(x,t)$ at which the solution is desired, to the decremented time $(t - \Delta t)$ where the solution is known. Along the characteristics, which are approximated locally by straight lines, the compatibility conditions are integrated using a modified Euler predictor-corrector method. For a detailed discussion of the method, see [34]. The second order derivatives appearing in the non-homogeneous term $\mathbf{C}$ are approximated by simple finite difference expressions.

SOME COMMENTS ON THE BOUNDARY CONDITIONS. — In all the 'deterministic' numerical simulations, the sandpile is imagined to be bounded by a wall on the left at $x = 0$, and a sink on the right at $x = L$, as depicted in figure 3. The background slope S_c is always taken as zero. Finally, there is always a source of grains η, in this case, of 'hard grains' added somewhere on the pile, either as a pulse, or as a constant flux. Since there are two second order partial

derivatives in the governing equations, we require four boundary conditions in all, at $x = 0$ and $x = L$. These are prescribed as follows.

i) At $x = L$, we assume that no cliffs can occur, i.e., the height $h(L,t) = 0$. This is consistent with our equations, which would relax such a shock rapidly (see Sect. 2.1).

ii) The existence of a sink at $x = L$ implies that the rolling grains arriving at $x = L$ are immediately removed. Thus $\mathcal{R}(L,t) = 0$.

iii) The net flux of grains from the left must be zero due to the presence of the wall. Thus at $x = 0, v\mathcal{R} - \mathcal{D}\partial_x\mathcal{R} = 0$.

iv) We assume that the gradient of h at the wall, $\partial_x h = 0$. One might anticipate that perhaps there exists for powders, as in the case of liquids, a 'wetting angle' at the wall, such that, $\partial_x h(x = 0)$, is some physical constant $k \neq 0$ depending on the nature of the wall, and the powder grains. In the absence of precise information, we have chosen the value $k = 0$ above. In any case, our results are expected to be independent of the precise choice of this constant.

The use of a scheme derived from the Method of Characteristics, requires that all the variables be prescribed on the initial curve. The height $h(x,0)$ has been assumed to be a parabola, starting with zero slope at some value $h(0,0)$ at $x = 0$, and decreasing to zero at $x = L$, consistent with the boundary conditons (i) and (iv) above. The rolling grains are supposed to not exist initially, i.e. $\mathcal{R}(x,0) = 0$ (consistent with (ii) and (iii) above). However, the nature of the governing equations ensures that they are generated at the very first time step due to the influx of grains on the pile, either at the top or at the bottom.

As mentioned in the previous section, the second order derivatives are treated as the inhomogeneous part of a set of first order equations. The numerical scheme adopted here then requires that they be prescribed at every point x, at the time $(t - \Delta t)$ in order that the solution at time t be obtained. Except at the boundary points, they are obtained from a simple finite difference formula. At the boundaries however, they are estimated as follows.

i) Since $\mathcal{R} = 0$ at $x = L$,

$$\kappa\mathcal{R}\partial_x^2 h = 0$$

and, the equation for $\mathcal{R}(x,t)$ implies,

$$\mathcal{D}\partial_x^2\mathcal{R} = v\partial_x\mathcal{R} - \eta$$

ii) Once the interior derivatives are calculated with a finite difference scheme, then one can use a Taylors series expansion to find,

$$\mathcal{D}\partial_x^2\mathcal{R}(x = 0) = 2\mathcal{D}\partial_x^2\mathcal{R}(x = \Delta x) - \mathcal{D}\partial_x^2\mathcal{R}(x = 2\Delta x)$$

Finally, at $x = 0$, one can use the compatibility condition equation (A-4) to find $\kappa\mathcal{R}\partial_x^2 h$ at t, from the known solution at $(t - \Delta t)$. At $t = 0$, this term is zero, since $\mathcal{R} = 0$.

References

[1] Bagnold R.A., 'The Physics of Blown Sand and Desert Dunes', (Methuen, London 1941), *Proc. Roy. Soc. A* **225** (1954) 49;
Brown R.L., Richard J.C., 'Principles of Powder Mechanics' (Pergamon, New York, 1966).

[2] Jenike A.W., 'Storage and Flow of Solids', Bulletin 123 (Univ. Utah Engg. Expt. Station, 1964);
Prakash J. R., Rao K.K., *J Fluid Mech.* **225** (1991) 21;
Marchello J.M., 'Gas-Solids Handling in the Process Industries', J.M. Marchello, A. Gomezplata

Eds. (Marcel Dekker, 1976);
Shamlou P.A., 'Handling of Bulk Solids' (Butterworths, 1988).
[3] Bak P., Tang C., Wiesenfeld K., *Phys. Rev. Lett.* **59** (1987) 381; *Phys. Rev. A* **38** (1988) 364.
[4] Jaeger H.M., Liu C.H., Nagel S.R., *Phys. Rev. Lett.* **62** (1989) 40.
[5] Evesque P., Rajchenbach J., *Phys. Rev. Lett.* **62** 44 (1989);
Douady S., Fauve S., Laroche C., *Europhys. Lett.* **8** (1989) 621.
[6] Held G.A., Solina D.H., Keane D.T., Haag W.J., Horn P.M., Grinstein G., *Phys. Rev. Lett* **65** (1990) 1120;
Grumbacher S.K., McEwen K.M., Halvorson D.A., Jacobs D.T., Lindler J., *Am. J. Phys.* **61** (1993) 329.
[7] Rajchenbach J., *Phys. Rev. Lett.* **65** (1990) 2221.
[8] Bak P., Creutz M., 'Fractals and Disordered Systems', vol. II, A. Bunde and S. Havlin Eds. (Springer Verlag, 1993).
[9] see e.g. Majumdar S.N., Dhar D., *Physica A* **185** (1992) 129 and references therein.
[10] Thompson P.A., Grest G.S., *Phys. Rev. Lett* **67**(1991) 1750;
Lee J., Herrmann H., *J. Phys. A.* **26**(1993) 373;
Herrmann H.J., *Physica A* **191** (1991) 263.
[11] Nagel S.R., *Rev. Mod. Phys.* **64** (1992) 321.
[12] Jaeger H.M., Liu C.H., Nagel S.R., Witten T. A., *Europhys. Lett.* **11** (1990) 619.
[13] Kadanoff L.P., Nagel S.R., Wu L., Zhou S.M., *Phys. Rev. A* **39** (1989) 6524.
[14] Hwa T., Kardar M., *Phys. Rev. Lett.* **62** (1989) 1813; *Phys. Rev. A* **45** (1992) 7002. Note that these papers were primarily aimed at describing the 'toy' sandpiles of [3] more than to model faithfully 'real' sandpiles.
[15] de Gennes P.G. (1989, unpublished).
[16] Mehta A., Needs R.J., Dattagupta S., *J. Stat. Phys.* **68** (1992) 1131;
Mehta A., Barker G., *Phys. Rev. Lett.* **67** 394 (1991); to be published in *Rep. Prog. Phys.*;
Mehta A., 'Granular Matter', A. Mehta Ed. (Springer, 1994) and references therein.
[17] Forster D., Nelson D., Stephen M., *Phys. Rev A* **16** (1977) 732 .
[18] Medina E., Hwa T., Kardar M., Zhang Y., *Phys. Rev. A* **39** (1989) 3053.
[19] Schwartz M., Edwards S.F., *Europhys. Lett* **20** 301 (1992);
Bouchaud J.P., Cates M.E., *Phys. Rev. E* **47** (1993) 1455 and *Erratum* **48** (1993) 635;
Prakash J.R., Bouchaud J.P, Edwards S.F., *Proc. Roy. Soc.* **446** (1994) 67.
[20] Kardar M., Parisi G., Zhang Y., *Phys. Rev. Lett.* **56** (1986) 889.
[21] for an introduction, see: Vicsek T., 'Fractal Growth Phenomena' (World Scientific, 1991);
Krug J., Spohn H., 'Solids Far From Equilibrium', C. Godrèche Ed. (Cambridge, 1992).
[22] see e.g. Prigogine I. , Herman R., 'Kinetic theory of vehicular traffic' (Elsevier, NY, 1971);
and some more recent papers: Nagel K., Schreckenberg M., *J. Phys. I France* **2** (1992) 2221;
Nagatani T., *J. Phys. A.* **26** (1993) L1015;
Kerner B., Konhauser P., *Phys. Rev. E* **48** (1993) 2335.
[23] Pak H.K. and Behringer R.P., *Phys. Rev. Lett.* **71** (1993) 1832;
Nagel S.R., private communication.
[24] We in fact considered situations where the slope goes smoothly to zero for $x = 0$ to satisfy our boundary conditions - See Appendix.
[25] Bagnold R.A., *Proc. Roy. Soc. A* **295** (1966) 219.
[26] Evesque P., private communication and in preparation.
[27] Note that the transition exhibits strong hysteresis, which can be understood within our model through the dependence of the flushing time T on the level of noise $\Delta\mathcal{R}_0$: sustaining avalanches is thus easier than triggering them.
[28] Numerical Recipes, (W.H. Press, B.P. Flannery, S.A. Teukolsky, W.T. Vetterling) (Cambridge University Press, 1986).
[29] Edwards S.F., Wilkinson D., *Proc. Roy. Soc. A* **381** (1982) 17.
[30] Equation (13) is strictly speaking valid in the limit of large local Peclet numbers: $\gamma a/\kappa$ and $va/\mathcal{D} \gg 1$.

[31] see e.g. Bouchaud J.P., Georges A., *Phys. Rep.* **195** (1990) 127, ch. IV.
[32] Prasad P., Ravindran R., 'Partial Differential Equations' (Wiley Eastern, 1985).
[33] Courant R., Hilbert D., 'Methods of Mathematical Physics', Vol. 2 (Interscience, 1962).
[34] Zucrow M.J., Hoffman J.D., 'Gas Dynamics', Vol. 2 (John Wiley, 1976).